International Journal of Engineering Research and Technology.
ISSN 0974-3154 Volume 11, Number 10 (2018), pp. 1485-1498

http://www.irphouse.com

Position Control of a Hummingbird Quadcopter Augmented by Gain Scheduling

Ngoc Phi Nguyen
Department of Aerospace Engineering,
Sejong University, Seoul, Republic of Korea, 05006

Sung Kyung Hong
Department of Aerospace Engineering,
Sejong University, Seoul, Republic of Korea, 05006

ABSTRACT

In this paper, a proportional derivative gain scheduling (PD-GS) approach that can control the position of a quadcopter in outdoor conditions is presented. The advantage of this method is smooth tracking, simple to implement in real-time applications, and wind rejection for position performance. The mathematical model of an unmanned quadcopter in the inertial frame has been provided to design appropriate controller for the quadcopter UAV. The response between proposed PD-GS controller and conventional one is compared through simulation and experiment results. The achieved results present the effectiveness of proposed approach.

Key Words: Position Controller, Gain Scheduling, PD Controller, Quadcopter, Wind Rejection.

I. INTRODUCTION

Quadcopter unmanned aerial vehicles (UAVs) are being increasingly employed in a variety of applications, such as military, aerial photography, delivery, and search-and-rescue operations. This is because they have advantages of small size, low cost, hovering ability, mechanical simplicity, agility, maneuverability, and indoor and outdoor operation, which makes them more interesting compared to other UAVs.

Various UAV development technologies have been investigated in recent years, such as target tracking control [1–2], fault diagnosis and fault tolerant control [3–4], and formation flight with multiple agents [5–6]. Development of such technologies requires use of the position controller in open source software. Although several control methods for quadcopter UAVs have been previously investigated [7–11], the proportional-derivative (PD) controller remains the most well-known for commercial purposes owing to its simple structure, real-time implementation, and no requirement of a mathematical model during the design phase. In fact, many renowned companies, such as Ascending Technologies [12], 3D Robotics [13], and AR Drone [14], employ the fixed-gain PD controller for position performance. However, these commercial controllers are challenging to smooth tracking and wind disturbance under windy conditions because their controller gains are unchanged during operation. Therefore, they need to be retuned for different situations.

Many existing papers have been studies control approaches on quadcopter UAV to reject the wind disturbances. Sahul et al. [15] developed a PID controller based on an optimization technique to eliminate wind disturbances. Gautam and Ha [16] presented a method that employs a fuzzy PID controller combined with EKF to reject wind disturbances during UAV position control. Another advanced approach was proposed by Cabecinhas et al. [17]. They designed a nonlinear adaptive controller to eliminate constant force disturbances. Other researchers have utilized estimation methods to estimate wind-disturbance forces and use them in conjunction with the controller. In [18], the wind effect was estimated using accelerometer data. This information was then used to improve the performance of the controller under presence of the wind effect. Madani and Benallegue [19] investigated UAV-tracking control in the presence of wind disturbances by employing a sliding-mode observer to estimate velocities and external disturbances. Additionally, a back-stepping controller was designed to compensate for modeling errors. In [20], when performing wind estimation, static as well as dynamic wind conditions were rejected using the control strategy based on adaptive and sliding-mode control methods. To design better wind-resistant controllers, researchers [21–22] have also investigated the use of onboard sensors as an information for the controller. The above methods, however, require intensive computation on part of the system, and are, therefore, not suitable for real-time implementation which uses low-cost microcontroller units for UAVs.

The proposed study presents a simple and effective control method for improving position-control performance of quadcopter UAVs. A PD-GS approach has been developed based on conventional PD to control the position of quadcopter UAVs. Advantages of this method include smooth tracking, less computation in real-time applications, and capability of reducing wind disturbances. The remaining of this paper is as follows. The dynamics of the quadcopter UAV is presented in Section 2. Section 3 subsequently describes controller design. Results obtained from the study are presented in Section 4 facilitating comparison between the proposed and PD approaches. Lastly, conclusion is presented in Section 5.

II. DYNAMICS OF QUADCOPTER UAV

The geometric configuration of the quadcopter with regard to the placement of motors and propellers is depicted in Fig. 1. The back and front motors (1 and 2) rotate in the counter-clockwise direction while motors 3 and 4 rotate in the opposite (clockwise) direction.

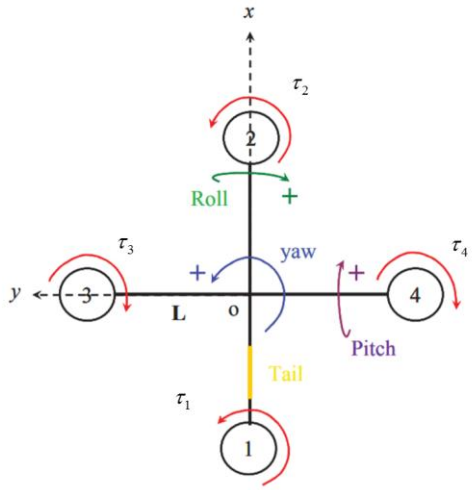

Fig. 1 Geometric configuration of the quadcopter UAV.

The four control variables can be defined as follows:

$$\begin{aligned} U_1 &= F_1 + F_2 + F_3 + F_4 \\ U_2 &= (F_3 - F_4)L \\ U_3 &= (F_1 - F_2)L \\ U_4 &= \tau_1 + \tau_2 - \tau_3 - \tau_4 \end{aligned} \tag{1}$$

where L is arm length; τ_i represents the torque produced by the ith motor; and F_i represents the thrust force generated by the ith propeller.

The thrust force and torque have relationships with the rotational speed of the propeller:

$$\begin{aligned} F_i &= b\Omega_i^2 \\ \tau_i &= d\Omega_i^2 \end{aligned} \tag{2}$$

where b, d represent the thrust and drag coefficients; Ω_i^2 represents the rotational speed of the ith motor.

Substituting equations (2) in (1) yields:

$$\begin{aligned} U_1 &= b(\Omega_1^2 + \Omega_2^2 + \Omega_3^2 + \Omega_4^2) \\ U_2 &= bL(\Omega_3^2 - \Omega_4^2) \\ U_3 &= bL(\Omega_1^2 - \Omega_2^2) \\ U_1 &= d(\Omega_1^2 + \Omega_2^2 - \Omega_3^2 - \Omega_4^2) \end{aligned} \tag{3}$$

Since rotor inertia is relatively small, low-speed quadcopter dynamics, in several extent studies [23–24], have been described as follows:

$$\begin{cases} \ddot{x} = \left\{U_1\left(\cos\phi\sin\theta\cos\psi + \sin\phi\sin\psi\right) + f_x\right\}/m \\ \ddot{y} = \left\{U_1\left(\cos\phi\sin\theta\cos\psi - \sin\phi\cos\psi\right) + f_y\right\}/m \\ \ddot{z} = \left\{U_1\left(\cos\phi\cos\theta\cos\psi\right) + f_z\right\}/m \\ \ddot{\phi} = U_2 / I_{xx} \\ \ddot{\theta} = U_3 / I_{yy} \\ \ddot{\psi} = U_4 / I_{zz} \end{cases} \tag{4}$$

Here x, y and z represent position coordinates of the quadcopter in the inertial frame; m is the quadcopter mass; ϕ, θ and ψ represent the roll, pitch, and yaw angles; I_{xx}, I_{yy} and I_{zz} represent the moments of inertia along the x, y and z directions; f_x, f_y and f_z represent wind forces.

III. CONTROLLER DESIGN

III.1 ATTITUDE CONTROLLER

This section describes the PD control law to control attitude of quadcopter. The control variable obtained using the PD control law can be expressed as:

$$U_2 = k_1\left[k_2\left(\phi_d - \phi\right) - \dot{\phi}\right] \tag{5}$$

where k_1, k_2 represent controller gains; ϕ_d is the desired roll angle; ϕ is the current roll angle; $\dot{\phi}$ is the current roll rate.

Fig 2 describes a schematic of the roll controller

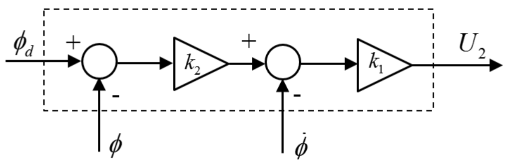

Fig. 2 Roll controller.

From (4) and (5), it can be demonstrated that:

$$\ddot{\phi} + \frac{k_1}{I_{xx}}\dot{\phi} + \frac{k_1 k_2}{I_{yy}}\phi = \frac{k_1 k_2}{I_{yy}}\phi_d \tag{6}$$

Let:

$$\begin{aligned} K_d &= k_1 / I_{xx} \\ K_p &= k_1 k_2 / I_{xx} \end{aligned} \tag{7}$$

Substituting (7) into (6), we get:

$$\ddot{\phi} + K_d \dot{\phi} + K_p \phi = K_d \phi_d \tag{8}$$

Standard form of the second-order system given by:

$$H(s) = \frac{\omega_n^2}{s^2 + 2\xi\omega_n s + \omega_n^2} \tag{9}$$

where ξ indicates damping ratio, ω_n indicates natural frequency, s denotes the Laplace operator.

The criteria of system is created as

$$\begin{aligned} t_s &= \frac{4}{\xi\omega_n} \\ M_p\% &= e^{-\frac{\pi\xi}{\sqrt{1-\xi^2}}} \times 100\% \\ t_r &= \frac{1.8}{\omega_n} \end{aligned} \tag{10}$$

where $M_p\%$ indicates the percentage of overshoot; t_s and t_r indicate the settling and rising times.

Combining (8) and (9) yields the controller gains as:

$$\begin{aligned} K_d &= 2\xi\omega_n \\ K_p &= \omega_n^2 \end{aligned} \tag{11}$$

Once K_p and K_d are obtained, controller gains k_1 and k_2 will be obtained from equation (7). The same approach is designed for pitch and yaw controller.

III.2 POSITION CONTROLLER

The objective of the proposed PD–GS controller is to not only achieve smooth tracking performance using the conventional PD-controller gains but also achieve good performance when operation in the position hold mode, which utilizes gain scheduling to reject wind disturbances. Fig 3 depicts a schematic of the proposed PD–GS approach, wherein the control system is based on the PD algorithm. The proportional and derivative gains are tuned via a gain scheduling operation, which is determined by the changing natural frequency ω_n. Prior to using the gain-scheduling operation, the PD controller must be designed.

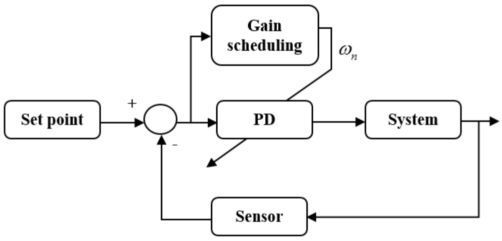

Fig. 3 Operating principle of the PD–GS approach.

The position dynamic equations used in the proposed approach can be rewritten as:

$$\begin{bmatrix} \ddot{x} \\ \ddot{y} \\ \ddot{z} \end{bmatrix} = \frac{1}{m} \begin{bmatrix} T_x \\ T_y \\ T_z \end{bmatrix} - \begin{bmatrix} 0 \\ 0 \\ g \end{bmatrix} \tag{12}$$

where T_x, T_y and T_z represent virtual control variables in the x, y and z directions, respectively.

Considering motion in the z direction, we have

$$\ddot{z} = \frac{T_z}{m} - g \tag{13}$$

Let

$$T_z = mg + T_1 \tag{14}$$

From equations (13) and (14), it can be shown that:

$$\ddot{z} = \frac{T_1}{m} \tag{15}$$

The PD control law for motion along the z direction can be described as:

$$T_1 = k_{1z}\left(k_{2z}\left(z_d - z\right) - \dot{z}\right) \tag{16}$$

where k_{1z}, k_{2z} represent controller gains, z_d is the desired altitude, z is the current altitude, and $\dot{z}$ is the current vertical velocity.

Fig 4 describes a schematic of the z controller

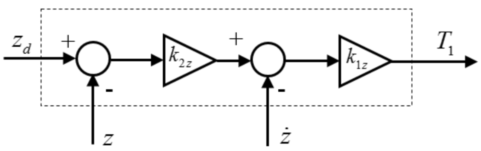

Fig. 4 Schematic of z controller.

From (15) and (16), one can obtain:

$$\ddot{z} = \frac{k_{1z}\left(k_{2z}\left(z_d - z\right) - \dot{z}\right)}{m} \tag{17}$$

Let:

$$\begin{aligned} K_{dz} &= k_{1z} / m \\ K_{pz} &= k_{1z} k_{2z} / m \end{aligned} \tag{18}$$

From (17) and (18), the following result can be obtained:

$$\ddot{z} + K_{dz}\dot{z} + K_{pz} z = K_{pz} z_d \tag{19}$$

Equation (19) can be considered as a second-order system. The controller gains K_{pz}, K_{dz} can be obtained as follows:

$$\begin{aligned} K_{dz} &= 2\xi\omega_n \\ K_{pz} &= \omega_n^2 \end{aligned} \tag{20}$$

It is obvious from equations (18) and (20) that in order to obtain controller gains k_{1z} and k_{2z}, the natural frequency ω_n and damping ratio ξ need to be tuned. The position controller has been designed with a damping ratio ξ equal to 0.7. The natural frequency ω_n is adjusted using the absolute error, as shown in Fig 5. If the absolute error $|e|$ exceeds a certain value e_0, the natural frequency is held constant at the same value as for the PD controller case for tracking performance. When operating in the position hold region, however, the natural frequency can be adjusted to tune controller gains using the following equation:

$$\omega_n = c.|e| + d \tag{21}$$

where c and d are two constants that need to be determined.

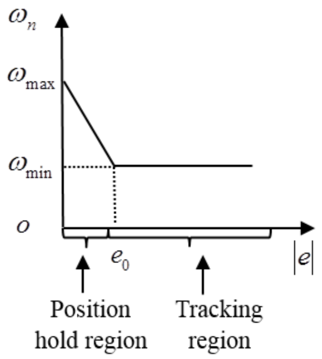

Fig. 5 Principle of the gain scheduling operation.

It is noticed from equation (21) that the natural frequency need to be satisfied

$\omega_{\min} \le \omega_n \le \omega_{\max}$ to get robust performances for controller. The same approach is applicable to controllers in the x, y directions.

The control variable U_1 is denoted as:

$$U_1 = \frac{T_z}{\cos\phi\cos\theta} \tag{22}$$

The desired roll and pitch angles can be obtained as follows:

$$\begin{bmatrix} \theta_d \\ \phi_d \end{bmatrix} = \frac{1}{U_1}\begin{bmatrix} \cos\psi_d & \sin\psi_d \\ -\sin\psi_d & \cos\psi_d \end{bmatrix}\begin{bmatrix} T_x \\ T_y \end{bmatrix} \tag{23}$$

IV. SIMULATION STUDY AND EXPERIMENTAL RESULTS

IV. SIMULATION STUDY

To verify the performance of the position controller in the horizontal direction, the PD control law and the PD-GS are applied to the dynamic model that presented in equation (4). The conventional PD approach was employed with a damping ratio of 0.7 and natural frequency of 0.6 rad/s. For the PD–GS approach, the damping ratio was held constant at 0.7 while the natural frequency was defined as follows:

$$\omega_n = \begin{cases} 0.6 & if \quad |e| > 2 \\ -0.5|e| + 1.6 & if \ 0 < |e| \le 2 \end{cases} \tag{24}$$

Design specifications of the Hummingbird Quadcopter are listed in Table 1.

Table 1 Design specifications of Hummingbird Quadcopter.

Parameter	Symbol	Value	Units
Mass	m	0.616	kg
Arm Length	L	0.17	m
Inertia moment of x-axis	I_{xx}	0.0073	$kg.m^2$
Inertia moment of y-axis	I_{yy}	0.0073	$kg.m^2$
Inertia moment of z-axis	I_{zz}	0.0117	$kg.m^2$

Fig 6 compares the performance of the conventional PD and PD–GS approaches along the x direction in the presence of the wind force depicted in Fig 7. Performances of the two approaches mentioned above were evaluated using the quadratic error index given by:

$$I_{qe} = \int_0^t e(t)^2 dt \tag{25}$$

The quadratic error index calculated from $t = 9.55\,s$ for each approach is listed in Table 2.

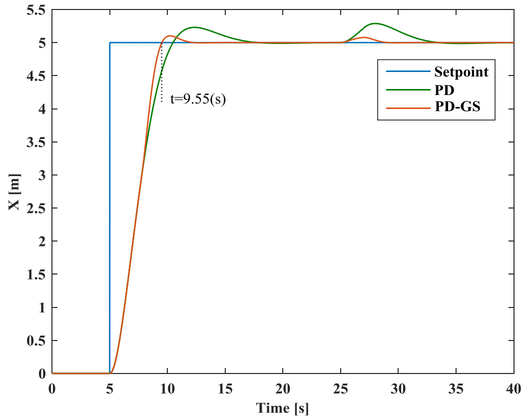

Fig. 6 Comparison of conventional PD and PD–GS approaches in the presence of wind force.

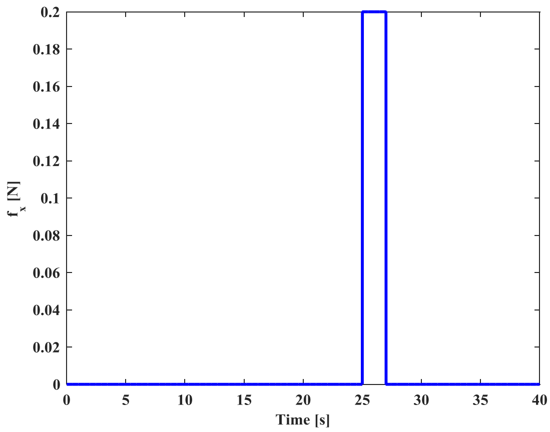

Fig. 7 Wind force acting along the x direction.

Table 2 Quadratic Error of Two Approaches

Algorithm	Quadratic error [m^2]
PD	43.677
PD–GS	2.021

Fig 8 compares the response between two controllers in circular path and rectangle path respectively under wind force acting x direction depicted in Fig 9.

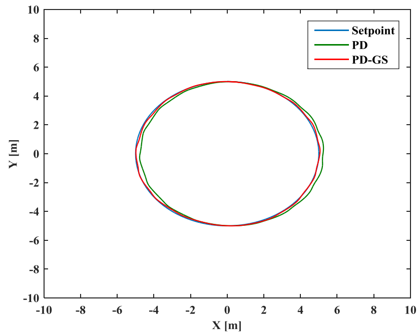

(a)

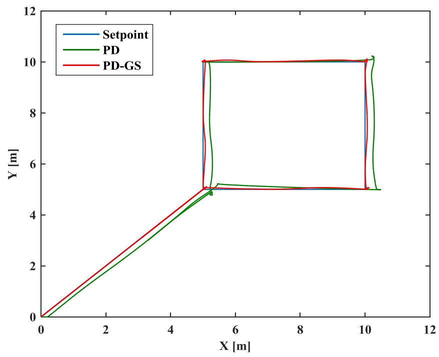

(b)

Fig. 8 Response between two approaches:
(a) in circular path, (b) in rectangle path

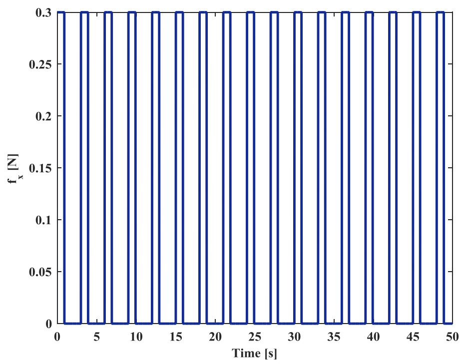

Fig. 9 Wind force acting along x direction

This results confirm that the proposed PD–GS approach-based controller demonstrates a better performance compared to the conventional PD controller in the presence of a wind force.

IV.2 EXPERIMENTAL RESULTS

The performance of the Hummingbird quadcopter was controlled by a combination of software and hardware. The ground control system was implemented in the MATLAB/Simulink environment to send commands to and receive flight data from the quadcopter via the Xbee wireless radio communication module. The attitude- and position-control algorithms were implemented onboard the high-level (HL) processor in the quadcopter. The attitude and position controllers were updated to frequencies of 1 kHz and 5 Hz, respectively. The experiment was divided into two parts. Initially, the command $z = 5\,\text{m}$ was issued by the user. After attainment of a stable altitude, the user issued the second command $x = 7\,\text{m}$, $y = 0\,\text{m}$. Fig 10 compares performance of position controller along the x and y directions, corresponding to the PD–GS and PD approaches. From time $t = 17.5\ s$ to the end of the experiment, the position hold performance for the two approaches are presented in Fig 11. The quadratic error index for each approach is listed in Table 3.

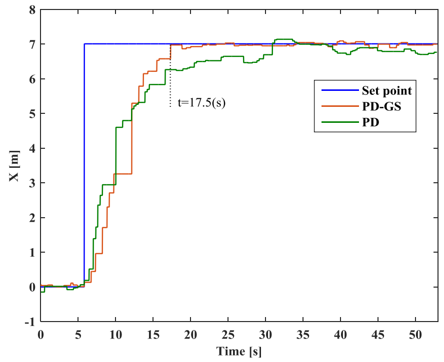

(a)

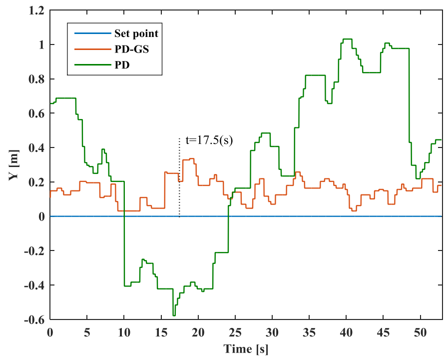

(b)

Fig. 10 The response of two approaches:

(a) in x direction, (b) in y direction

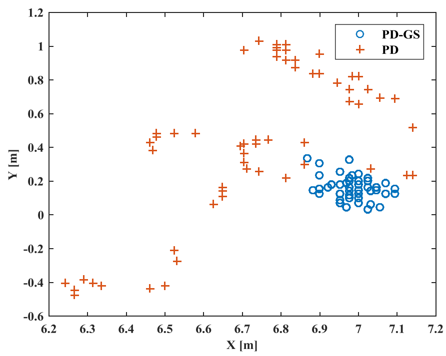

Fig. 11 Position hold performance between the two approaches.

Table 3 Comparison of Position-Controller Performance between Two Approaches

Algorithm	Quadratic error in x direction [m^2]	Quadratic error in y direction [m^2]
PD	221.0978	709.3147
PD–GS	5.3108	53.6539

The response of proposed controller is faster and quicker to return to position hold region compared to conventional one. Moreover, the proposed controller can also obtain smooth tracking from controller gains of conventional PD.

V. CONCLUSION

In this work, the quadcopter can be made to perform smooth maneuvers while in flight, the effect of wind disturbance has also been reduced. Moreover, this approach is straight forward to use in real-time implementation. However, the stability of system has not been addressed because the range of natural frequency depends on trial and error approach. This is solved in the future.

ACKNOWLEDGEMENT

This research was supported by the MSIT(Ministry of Science and ICT), Korea, under the ITRC(Information Technology Research Center) support program(IITP-2018-2018-0-01423) supervised by the IITP(Institute for Information & communications Technology Promotion)", and also it was partially supported by the National Strategic Project-Fine particle of the National Research Foundation of Korea(NRF) funded by MSIT, ME(Ministry of Environment), and MOHW(Ministry of Health and Welfare) under Grant 2017

REFERENCES

[1] W. Ren & R. W. Beard, Trajectory tracking for unmanned air vehicles with velocity and heading rate constraints, IEEE Transactions on Control Systems Technology, 12(5), 2004, 706–716.

[2] R. Bonna & J. F. Camino, Trajectory Tracking Control of a Quadcopter Using Feedback Linearization, Proceeding of the XVII International Symposium on Dynamic Problems of Mechanics, 2015, Brazil.

[3] N. P. Nguyen and S. K. Hong, Sliding Mode Thau Observer for Actuator Fault Diagnosis of Quadcopter UAVs, Applied Sciences, 8(10), 2018, 1893.

[4] F. Chen, W. Lei, G. Tao, & B. Jiang, Actuator Fault Estimation and Reconfiguration Control for Quad-rotor Helicopter, International Journal of

Advanced Robotic Systems, 13(33), 2016.
[5] W. Zhao and T. H. Go, Quadcopter formation flight control combining MPC and robust feedback linearization, Journal of Franklin Institute, 351(3), 2014, 1335-1355.
[6] A. Mahmood & Y. Kim, Decentralized formation flight control of quadcopters using robust feedback linearization, Journal of the Franklin Institute, 354(2), 2017, 852-871.
[7] E. Reyes-Valeria, R. Enriquez-Caldera, S. Camacho-Lara, & J. Guichard, LQR control for a quadcopter using unit quaternions: Modeling and simulation, International Conference on Electronics, Communications and Computing (CONIELECOMP), March 2013, 172–178.
[8] F. Rinaldi, S. Chiesa, & F. Quagliotti, Linear Quadratic Control for Quadcopters UAVs Dynamics and Formation Flight, Journal of Intelligent & Robotic Systems, 70(1-4), 2013, 203–220.
[9] I. Cowling, O. Yakimenko, J. Whidborne, & A. Cooke, A prototype of an autonomous controller for a quadcopter UAV, European Control Conference (ECC), 2007, 4001–4008.
[10] T. Madani & A. Benallegue, Backstepping Control for a Quadcopter Helicopter, IEEE/RSJ International Conference on Intelligent Robots and Systems (IROS), 2006, 3255–3260.
[11] S. Bouabdallah & R. Siegwart, Backstepping and Sliding-mode Techniques Applied to an Indoor Micro Quadcopter, IEEE International Conference on Robotics and Automation, 2005, 2259–2264.
[12] http://www.asctec.de/
[13] https://3dr.com/
[14] https://www.parrot.com/global/drones/parrot-ardrone-20-elite-edition
[15] M.P.V Sahul, V. N. Chander, & T. Kurian, a novel method on disturbance rejection PID controller for quadcopter based on optimization algorithm, Third International Conference on Advances in Control and Optimization of Dynamical Systems, 2014.
[16] D. Gautam, & C. Ha, Control of a Quadcopter Using a Smart Self-Tuning Fuzzy PID Controller, International Journal of Advanced Robotic Systems, 10, 2013.
[17] D. Cabecinhas, R. Cunha, and C. Silvestre, Experimental validation of a globally stabilizing feedback controller for a quadcopter aircraft with wind disturbance rejection, American Control Conference (ACC), 2013, 1024–1029.
[18] S. Waslander & C. Wang, Wind Disturbance Estimation and Rejection for Quadcopter Position Control, AIAA Infetech@Aerospace Conference, Apr 2009.
[19] T. Madani & A. Benallegue, sliding mode observer and backstepping control

for a quadcopter unmanned aerial vehicles, American control conference, 2007.
[20] J. Escareño, S. Salazar, H. Romero, & R. Lozano, Trajectory control of a quadcopter subject to 2D wind disturbances, Journal of Intelligent & Robotic Systems. 2013; 51-63.
[21] D. Yeo, N. Sydney, D. A. Paley, & D. Sofge, Onboard Flow Sensing for Downwash Detection and Avoidance with a Small Quadcopter Helicopter, AIAA Guidance, Navigation, and Control Conference, 2015.
[22] C. Lambert, M. Nahon, and D. Chalmers, Implementation of an aerostat positioning system with cable control, IEEE/ASME Transactions on Mechatronics, 12(1), 2007.
[23] W. Dong, G. Y. Gu, X. Zhu, & H. Ding, Modeling and control quadcopter UAV with aerodynamics concepts, International Journal of Mechanical, Aerospace, Industrial, Mechatronic and Manufacturing Engineering, 7(5), 2013.
[24] Y. Zhang & A. Chamseddine, Fault tolerant flight control techniques with application to a quadcopter UAV testbed, Automatic Flight Control Systems, 2012, DOI: 10.5772/3891.